Outlet glacier and margin elevation changes: near-coastal thinning of the Greenland ice sheet

W. Abdalati[1], W. Krabill[2], E. Frederick[3], S. Manizade[3], C. Martin[3], J. Sonntag[3], R. Swift[3], R. Thomas[3], W. Wright[2], and J. Yungel[3]

[1]NASA Goddard Space Flight Center, Code 971, Greenbelt, MD 20771

[2]NASA Goddard Space Flight Center/Wallops Flight Facility, Code 972, Wallops Island, VA 23336

[3]EG&G Services, NASA Goddard Space Flight Center/Wallops Flight Facility, Code 972, Wallops Island, VA 23337

For Submission to Journal of Geophysical Research Atmospheres

Abstract

Repeat surveys by aircraft laser altimeter in 1993/4 and 1998/9 reveal significant thinning along 70% of the coastal parts of the Greenland ice sheet at elevations below about 2000 m. Thinning rates of more than 1 m/yr are common along many outlet glaciers, at all latitudes and, in some cases, at elevations up to 1500 m. Warmer summers along parts of the coast may have caused a few tens of cm/yr additional melting, but most of the observed thinning probably results from increased glacier velocities and associated creep rates. Three glaciers in the northeast all show patterns of thickness change indicative of surging behavior, and one has been independently documented as a surging glacier. There are a few areas of significant thickening (over 1 m/yr), and these are probably related to higher than normal accumulation rates during the observation period.

Introduction

Outlet glaciers are particularly important to the mass balance of the Greenland ice sheet because they are the means by which the ice is discharged into the surrounding seas. Such discharge comprises nearly half of the ice sheet mass loss [Weidick, 1995]. An understanding of the balance of the glaciers themselves, and the mechanisms that affect this balance is essential to understanding the present and future states of the ice sheet. The factors affecting outlet glacier balance are complex, because their state of balance is not simply a result of accumulation and surface ablation, but rather the balance is largely influenced by flow characteristics, which are often non-linear.

Until recently, large-scale assessment of glacier mass balance was not possible by conventional means. While in situ measurements can provide detailed information about very specific locations, large-scale coverage is often not feasible because of the costs, difficulties, and dangers associated with work on these remote glaciers. Satellite radar altimetry has enabled the study of the higher portions of the ice sheet, but is limited to the shallow-sloped and relatively smooth areas and provides no useful information about the steeper areas closer to the coast. The Geoscience Laser Altimeter System (GLAS) aboard NASA's Ice Cloud and land Elevation Satellite (ICESat), scheduled for launch in 2001, will extend satellite coverage toward the coast and effectively measure elevation change characteristics over most of the main ice sheet. It will provide limited information on most of Greenland's outlet glaciers, which are comparatively narrow and sinuous, but in general, laser tracks will cross the glaciers at separations of up to seven kilometers in southern Greenland and roughly 2 km in the north. Extensive measurements of these outlet glaciers can be effectively made, however, through the use of airborne laser altimetry and precise global positioning system (GPS) techniques. Because of the maneuverability of aircraft platforms, such airborne surveys can be made along and across many glaciers at various time intervals and spatial separations.

In recent years results from NASA's Arctic Ice Mapping (AIM) missions using NASA's Airborne Topographic Mapper (ATM) laser altimeter have demonstrated that the upper reaches of the ice sheet, in excess of 2000 meters elevation, are essentially in balance [Krabill et al., in press]. This result is confirmed by an independent method that compares net mass input above 2000 meters to measured fluxes along the 2000 m contour line, and it is also in agreement with satellite radar altimetry observations [Thomas et al., submitted]. ATM results also indicate that there is significant thinning at elevations below 2000 m. The net deficit is estimated to be over 50 km^3 of ice per year, and at the lower elevations is assumed to be attributable to creep thinning [Krabill et al., in press].

These thinning rates increase closer to the coast, and are highest for the outlet glaciers through which most of the ice is channeled prior to discharge. In this investigation, we examine elevation changes measured on major outlet glaciers and less active ice margins (Fig. 1) to infer their state of balance, and we discuss the possible causes for these changes.

Outlet Glacier Change Mechanisms

In general, a glacier is thickened by snow accumulation and advection of thicker ice from upstream, and is thinned by surface and basal melting and by creep deformation of the ice. Except for floating glaciers, basal melting is small. Surface melting is strongly determined by summer temperatures, and snow accumulation by weather patterns. Consequently, both are highly variable from year to year, and this natural variability causes the ice to thicken and thin. Averaged over many years, melt and accumulation show less (but not zero) variability, and a "steady-state" glacier is one that is in balance with its long-term variability.

To interpret glacier changes over a discrete measurement interval, melting, accumulation, and flow rates and their variability need to be considered. Melting rates are strongly linked to the positive-degree-days (PDD's), defined as the product of days (or fractions of days) with temperatures greater than 0°C times the number of degrees in excess of 0°C. The relationship between PDD and ablation is assumed to be proportional, and is generally approximated by a regionally specific proportionality constant. Anomalous melting can be inferred from anomalies in local PDD, which can readily be estimated from regular observations at coastal weather stations, after adjustment for an appropriate lapse rate.

By contrast to the simple melt model, accumulation variability is a consequence of large-scale atmospheric circulation that must be simulated by sophisticated weather models. Precipitation rates at coastal stations are both unreliable, and poorly representative of conditions on nearby areas. Consequently, definitive estimates of interannual snow accumulation variability have historically been limited to inferences made from careful analysis of ice core stratigraphy (McConnell et al., 2000). In addition, model simulations of such variability are becoming increasingly reliable as spatial resolution and physical realism of the models improve (Bromwich et al., this issue). Both of these methods, however are problematic near the coast where reliable cores cannot be acquired, local topography is extreme, and models cannot be validated.

Ice velocity and creep rates are generally assumed to change slowly with time, but this assumption is based on very few measurements, and some glaciers experience cycles during which they thicken as they move too slowly to balance snow accumulation, with periodic brief "surges" when velocities and deformation rates increase by orders of magnitude, resulting in massive thinning. Such behavior is controlled largely by glacial geometry and basal characteristics (Paterson, 1994; van der Veen, 1999], and the time period between surges is unique for each glacier.

Arctic Ice Mapping (AIM) Program

The Arctic Ice Mapping program began in 1991 with some initial laser-altimetry elevation surveys along the western flank of the Greenland ice sheet. When it became apparent that the surveys were sufficiently accurate to detect ice sheet elevation changes, a comprehensive plan was developed for large-scale airborne assessment of elevation changes. The intent was to determine the current ice sheet mass balance and to identify areas of positive and negative balance. Under the plan, the ice sheet was surveyed extensively along carefully planned flight lines in 1993 and 1994, and again along the same flight lines five years later. The southern portions (south of 71°N) were surveyed in 1993 and again in 1998, while the northern regions were surveyed in 1994 and 1999. During the intervening years, additional surveys were performed in support of other research activities.

The instruments used for the AIM surveys are two versions of the Airborne Topographic Mapper (ATM-1 and ATM-2) flown on the NASA P-3B Orion aircraft. These sensors combine high pulse-rate laser ranging (up to 5000 Hz) with a scanning capability [Krabill et al., 1995]. The ATMs are currently operated with Spectra Physics TFR laser transmitters, which provide a 250 μJ pulse that is 7ns wide at a frequency-doubled wavelength of 523 nm in the blue-green spectral region, or with Continuum EPO5000 transmitters, which provide a 125 μJ pulse that is 1.5ns wide at a frequency-doubled wavelength of 532 nm, also in the blue-green spectral region. The scanning is achieved with a nutating mirror that directs the laser beam toward the surface in an elliptical pattern, resulting in a swath of measurements beneath the aircraft. ATM-1 scans at 10 Hz and 10° off-nadir, and ATM-2 scans at 20 Hz and 15° off-nadir. The swath width is nominally 140 to 250 meters for ATM-1 and ATM-2 respectively at a flight altitude of approximately 450 m above ground level (a.g.l.), with spot sizes on the order of 1 meter and separated by approximately 2-4 meters. This sampling facilitates repeat surveys by providing a relatively wide target for later overflights. In 1998, the original flight lines were repeated typically to within 50 m, allowing substantial overlap [Krabill et al., 1999].

Approach

The AIM missions have yielded excellent results over most of the ice sheet, identifying regions of thickening and thinning with unprecedented accuracy and spatial coverage. Results have been reported for the main parts of the ice sheet based primarily on interpolation of a smoothed version of the data [Krabill et al., 1999, Krabill et al., in press]. The outlet glaciers, and the rough margins, however, require detailed analysis of individual laser shots. For flight trajectories with data from two survey years, each laser shot from the earlier survey is compared with all shots within one meter to infer the change in elevation. The result is a dense array of elevation changes along a flight line that characterize the thickening or thinning of the ice in the intervening time.

To put the observed elevation changes into their proper context, annual average ablation rates are also examined for each of the outlet glaciers surveyed using the positive degree day (PDD) model [Reeh, 1991]. PDDs are calculated for any location on the ice sheet as a function of its latitude and elevation. The ablation is then determined by multiplying the PDD value by a factors of 0.003 and 0.008 m water per degree day for snow and ice respectively [Braithwaite, 1995]. Assuming a density of ice of 917 kg/m^3, and a snow density of 333 kg/m^3, these values both translate to surface elevation changes of 0.009

m/degree-day. These degree-day factors are highly variable, particularly in the case of snow because they are temperature-based and don't sufficiently account for variations in absorbed energy albedo changes during surface melt and metamorphism. For some locations, the factors for snow are as high as 0.022 m water/yr [Braithwaite, 1995], but these are generally limited to the higher regions on the main ice sheet and do not apply to the outlet glaciers. The factor 0.008 m water/yr is considered appropriate for the lower-elevation outlet glaciers and the ice margins.

It is important to note that a thinning rate equal in magnitude to the ablation rate does not imply that ablation is the dominant mechanism. To determine the relative role of ablation in the observed thinning, the *anomaly* should be considered. Under steady-state conditions, annual ablation is balanced out by accumulation; whereas the anomaly is a deviation from the climatological average conditions. We provide ablation estimates in order to present the observed changes in the context of the annual cycle; however, for the purpose of determining ablation contribution to dh/dt, we also present the calculated anomaly.

For all of the glaciers in Figure 1, except Ryder, we calculate the ablation anomaly based on a 20-year climate record from nearby coastal weather stations (Ryder was too far from any of the stations for a meaningful comparison.). These data are decoded by the National Center for Environmental Prediction (NCEP) and distributed by the National Center for Atmospheric Research (NCAR). The coastal station data were examined to determine the extent to which the summer temperatures of the 5-year survey separation period were anomalous. Positive-degree-day (PDD) anomalies were calculated using 6-hourly temperature data from coastal stations around the perimeter of Greenland dating back to 1979. Only stations with data in 15 of the last 20 years, and all 5 of the years that separate the surveys were used. PDD anomalies were calculated by subtracting the mean PDD for the full record from that for the 5-year period between surveys. The magnitudes of these anomalies were reduced linearly with elevation assuming that they were zero at an elevation of zero melt. This elevation was assumed to vary linearly from 2900 meters at 63°N latitude and 2000 m at 80°N latitude, based on the melt distribution of Abdalati and Steffen [1997].

Results and Discussion

The results are shown in Figures 2 through 7. They show spatially varying patterns of thickening and thinning of different outlet glaciers, with some regional coherence. Most glaciers thinned during the survey period, some by several meters per year, while a few show evidence of thickening. Some show substantial thinning in the lower reaches but considerable thickening in the upper areas, a behavior consistent with surge type glaciers. Results for each region are presented and discussed below.

Southeast (SE)

One of the more dramatic areas of thinning is the southeast region of the ice sheet. Six specific surveys were made (Figure 1). The three northernmost in the region are on conventional outlet glaciers (King Christian, Kangerdlugssuaq, and Helheim), with the flow clearly defined through a channel and into a fjord. The Topex survey, so named because it covers the 66° northern limit of the Topex orbit, is not over an outlet glacier, but rather is simply near the ice margin. The stagnant ice margins are significant to our study because in these locations, creep rates are very small, and mass losses are driven more by melt/runoff, sublimation and evaporation; hence they allow us to test the validity of our PDD approach to ablation. It is not clear whether the Ikerssuaq flight is over a glacier or an ice margin; however the region is crevassed, indicating some level of dynamic activity, and the ice extends to the land edge. The Pikiutdleq flight is along a glacier with a flow rate on the order of 1 km/yr [Abdalati and Krabill, 1999].

Results for each survey line in the region are shown in Figure 3. The most dramatic thinning can be found on Kangerdlugssuaq Glacier, with rates that approach 10 meters per year at some locations in the lower reaches. This thinning extends more than 70 km upslope from the calving front where it is still on the order of 1 meter per year. The sheer magnitude of these tremendous thinning rates clearly indicates that they are dynamic in nature rather than a result of melt or accumulation changes [Krabill et al., 1999, Thomas et al., 2000]. There are some gaps in the coverage, but the shape of the thinning curve (Figure 3) in the areas where there is coverage suggests that this behavior is maintained in the segments without data, and interpolation is possible. The resulting net imbalance for the glacier and its catchment region has been estimated at approximately 6 cu km per year [Thomas et al., 2000].

Similar thinning, though not as extreme, is occurring on Helheim Glacier (Figs. 2 and 3). Thinning rates range from a few tens of centimeters 200 km inland to nearly 1.5 m/yr within about 40 km of the calving front at 1200 m elevation. Because of gaps in the data, it is difficult to estimate the thinning behavior at lower elevations, but extrapolation from the up-glacier results, suggests a maximum of approximately 2 m/yr near the terminus.

The thinning extends much farther down the east coast with rates of 0.5 to 1 m/yr at the east/west flightline at 66°N (the northern limit of the TOPEX orbit) and the Ikerssuaq and Pikiudtleq regions. It is important to note that the Topex flight line, which is over relatively stagnant ice, shows dh/dt values that are consistent with the calculated ablation anomalies. Such a relationship for the fairly stagnant ice margins subject to minimum creep provides some validation for our PDD-based estimate of ablation anomaly. There is strong agreement between the observed dh/dt and the ablation anomaly, suggesting that thinning in this particular area may not be related to flow rates.

The consistent character of this thinning along each of the Southeast flight lines suggests a widespread mass loss in this entire southeast region. Analysis of other southern glaciers indicates that this widespread thinning is not limited to the Southeast.

South/Southwest (S)

Further south, data from the three flight lines in the King Frederick and Eqalorutsit region show thinning rates of 0.5 to 1 m/yr, yet they show a thickening at higher elevations (Fig. 4). In the case of the King Frederick line, the thickening may be a result of the crossing of the flightline over the ridge and into a different climate/hydrologic zone, since the ice sheet climate zones are primarily topographically defined. For the two in Eqalorutsit, however, the situation is more complex. The transitions from nearly 1 m/yr of thinning at lower elevations to areas of thickening at higher elevations occur over short distances (50-80 km).

The ablation anomaly was fairly high in the Eqalorutsit region, and the thinning associated with that anomaly is equal to the observed thinning at elevations ranging from 1600-2000 m and 1450-1700 m respectively (Fig. 4), but this does not explain the large thinning rates below these elevations or the thickening higher up. At the lower elevations, we assume creep thinning occurred at rates in excess of any ablation or accumulation effects, similar to the southeastern part of the ice sheet. The thickening at higher elevations may have been caused by increased accumulation.

The two remaining glaciers surveyed in the region are Kangiata Nunâta Sermia and Sarquap Sermerssua. The first shows enormous thinning rates of 4 m/yr near the terminus, well beyond the seasonal ablation rate. This diminishes to 0.5 m/yr upslope and 1100 m elevation, which is the modeled annual ablation rate. There was essentially no coastal temperature anomaly during the survey period, and the magnitudes of dh/dt at the lower elevations are far to large to be explained by precipitation anomalies, considering the annual precipitation rate is approximately 350 mmwe per year. Thus we believe that the thinning, particularly at the lower elevations, is likely to be dynamically driven. The ice near Sarquap Sermerssua shows a slight, but significant thinning near the terminus of about 0.5 m/yr but a substantial thickening further upslope. This transition is distinct at 700 m elevation (25-30 km from the calving front). Such behavior is consistent with the quiescent phase of glacier surging [Paterson, 1994]. There are no independent measurements to confirm this, and the magnitudes are small enough that the causes may be a result of local dynamics and accumulation and ablation variability, rather than a classic surge with velocities increasing by one or two orders of magnitude. In either case, it is unlikely that climate conditions differ over such a small distance, since there are no major topographic barriers separating the two portions of the transect.

Taken collectively, these southeastern and southwestern ice sheet observations offer compelling evidence that the most temperate regions of the ice sheet are diminishing considerably, most likely due to widespread creep rates caused by flow rates in excess of the balance velocities.

West (W)

The western flank of the ice sheet is characterized by relatively shallow slopes. As such, it is subject to extensive ablation, as well as relatively small driving stresses, when compared to the east coast and parts of the south. Despite this, five of the seven glaciers surveyed showed significant thinning on the order of tens of cm per year (Figure 5). One that did not was the Jakobshavn Isbrae, which thickened slightly. Because the Jakobshavn Isbrae may be responsible for 15-20% of the total ice sheet discharge [Weidick, 1995], its stability is particularly significant. Approximately 330 km north, the region of Giesecke Isfjord is showing slight thickening overall, with local areas of thinning near the ice edge. The presence of a warm anomaly in the region during the survey period indicates that the thickening is either a result of increased accumulation or glacier flow rates that are below the balance velocities. Our current information is insufficient to tell.

The other six glaciers in the area that were surveyed, Kangerdlugsuup Sermia, Rink Isbrae, Nunatakavasaup Sermia, Nansen Glacier, King Oscar Glacier, and Rink Glacier, show consistent thinning generally in excess of 50 cm/yr near the ice edge. These results indicate that for the most part, the region near the west coast between 72 and 77 degrees north latitude is undergoing widespread thinning, but with spots of local thickening. Because each of these areas in the west is generally subject to the same climate conditions [Ohmura and Reeh, 1991], the spots of thickening suggest that dh/dt is not dominated by ablation or accumulation, but flow imbalance that appears to be consistent over most of the glaciers surveyed in the vicinity.

North/Northwest (NW)

Coverage in this region (Figs. 2 and 6) is limited to Humboldt Glacier, a few small segments of Petermann Glacier, and a transect down Ryder Glacier with only two years separating the Ryder surveys. These results do show marked thinning near the edges of 2 segments of Humboldt Glacier. Features observed in ERS SAR imagery [© 1991, European Space Agency) from the region indicate that the northern line is over the fastest portions of the glacier. If the thinning were not flow-related, we would expect the two segments to behave similarly; however, if it were a result of a basin-scale increased creep rates, we would expect the faster portion of the glacier to thin more rapidly. Indeed the faster area is thinning at twice the rate. The last 150 km of the northern segment transitions from a steady-state condition to nearly 1 m/yr of thinning near the ice edge. The southern segment reaches a thinning rate of approximately 40 cm/yr. In addition, the PDD anomaly near the area was actually negative, indicating reduced ablation. In both the northern and southern lines, there is an apparent thickening at the end of the glacier where the ice is discharged into Kane Basin. The elevation curve flattens out in these regions indicating that they are areas of floating ice, so the observed thickening indicates that the response of the small ice shelf is lagging the input from the grounded ice. The result is a positive balance for the ice shelf, and potentially increased backpressure on the glacier. It is likely that this backpressure is mitigating the thinning of Humboldt Gletscher. The thickening of the ice shelf adjacent to a thinning glacier offers further evidence of flow-related rather than surface related causes for the thinning.

Petermann Glacier is subject to substantial ablation losses due to basal melting [Rignot, 1996], and believed to be part of a widespread negative balance in northern and northeastern Greenland [Rignot et al., 1997]. Unfortunately, the number of available repeat flights is limited to two flightlines, one of which is very discontinuous. Moreover, the two lines show different results. The southern one, which is more aligned with the glacier flow shows thinning of as much as 1 m/yr, but with some short sporadic areas of thickening by nearly the same amount. Such characteristics suggest either variable flow rates or migrating surface features. The distance between these extremes is on the order of 10 km, which points more to the latter than the former, but the details will require more extensive surveys. The more northerly survey indicates thickening of approximately 10 cm/yr. Based on the limited results, Petermann Glacier appears to be thinning overall, but even a very limited assessment cannot be estimated from these measurements.

Ryder Glacier experienced a "mini-surge" at the end of the 1995 melt season, in which velocities reached three times their normal values [Joughin et al., 1996]. Our Ryder Glacier surveys were made in 1997 and 1999, well after the mini-surge. The measurements show considerable scatter, where the ice is very rough, but the results do show evidence of local thickening and thinning. There is major thinning of 2 to 4 meters per year at approximately 52 km from the start of the flightline, where the elevation along the flow direction drops off rapidly. The bedrock topography at this steep drop off shows an abrupt rise of 450 meters over a distance of 3 km. This steep slope (0.15) is likely to act as a barrier to flow, which causes a buildup of backpressure that is released through enhanced discharge after a critical driving stress is reached or resistance to flow is reduced by bed lubrication. The flat character of the surface upstream from the 52 km mark may be a result of recent discharge, which would account for the observed thinning. This underlying topography may have contributed to the 1995 mini-surge. If the 1997-99 thinning is a result of similar short-duration enhanced discharge, this may be a frequently occurring event.

Just upslope of the thinning area is a thickening of approximately 0.5 m/yr followed by a thinning of nearly twice that magnitude. It is unclear why the dh/dt characteristics would exhibit such variability along the flight line, but one possible explanation is that enhanced flow may be local in nature and not experienced on the glacier as a whole. Further upslope at approximately 850 m elevation, an area thinned by nearly 7 meters per year (14 meters total). The elevation curve shows this to be a basin and a likely location of a supraglacial lake on the order of 5 km across (such lakes are evident in SAR imagery). It is likely that such a large elevation change in such a small area is a result of the draining or collapse of such a lake during the period between surveys. This behavior has also been observed by Joughin et al. [1996].

Northeast (NE)

The northeast shows widely varied behavior that is a result of glaciological and climatological differences within the region (Fig. 7) . The Kron Prins Christian ice dome has unique conditions of surface balance due to its situation with respect to the Northeast Water (NEW) polynya in the Greenland Sea. Moreover, it is subject to its own dynamic conditions, apart from the ice sheet, by virtue of its physical separation. The dome showed considerable thickening on the order of 0.5 m/yr in most locations, but as much as 3 m/yr in some others. This thickening is most likely related to relatively high levels of precipitation associated with more open water in the NEW polynya between the surveys than in the preceding years (L. Toudal, personal communication). The 3 m/yr thickening region is limited to a 10 km region on the Northwest side of the dome, and does not appear to be widespread. In winter, this is the leeward side of the dominant synoptic-scale circulation pattern, so it is possible that the thickening in this area results from a redistribution of mass deposited elsewhere on the dome.

A surge has been documented for Storstrommen Glacier between 1978 and 1984 [Reeh et al., 1995], and near zero velocities have been observed in the vicinity of the 100 m elevation contour [Reeh, et al., 1995]. Typical glacier behavior during quiescence is a thinning downstream of the start of the surge area, and a thickening upstream, as ice backs up in the vicinity of the velocity minima and does not replenish the outflow downstream. Such elevation change characteristics were observed for the Northern section of Storstrommen in the 1994/9 surveys (Fig. 7). Thinning of 2 m/yr in the lower reaches of the glacier (100 m elevation) was observed, but it diminishes and gives way to thickening of nearly 2.5 m/yr over a distance of 75 km. The entire upper reaches of the glacier are in positive balance.

The southern portion of Storstrommen glacier (flowing Northward from the south) show similar behavior, but of much smaller magnitude with thinning of 0.6 m/yr at 500 m elevation. These are similar in magnitude to the northern flight line down Storstrommen, but at higher elevations, the thickening rate is much less, approximately 10 cm/yr. We have no dh/dt measurements at elevations lower than 500 m, but if the thinning trend continues down the glacier, rates may be significantly greater. There is no documented surge in this glacier, but the rapid thinning, which is in excess of what would be expected from ablation or accumulation anomalies is consistent with enhanced discharge associated with surging.

Hagen glacier in the north also shows dh/dt characteristics that are consistent with surging behavior, with dh/dt values ranging from –3 m/yr to +2.5 m/yr over a distance of 20 km. There is considerable scatter between 0 and 10 km along the flight line, which is probably attributable to the presence of icebergs. At 35 km, there is a gap in coverage, but at 65 km, coverage is resumed again, and the elevation changes are fairly small, and consistent with that expected from the regional temperature anomalies.

Results from the remaining glaciers in the region are shown in Figure 7 and show very small elevation changes, which are likely to be a result of surface exchanges, considering their magnitude. Zacharaie Isstrom shows tremendous variability at areas below 400 m elevation. These areas have some relatively steep local slopes where driving stresses are high, and they are likely to be crevassed. The scatter can be attributed to elevations associated with the movement of crevasses. Heinkel Glacier appears to be thickening slightly (less than 10 cm/yr), and Wordie Glacier is thinning at a rate that only slightly exceeds the ablation anomaly.

Conclusions

The results of the laser altimetry repeat surveys provide insight to the balance characteristics of some of the major outlet glaciers. The general trend of dh/dt becoming increasingly negative in direct relation to coastal proximity indicates that the most substantial changes occur in the coastal regions and outlet glaciers. As nearly half of the ice sheet mass loss occurs through discharge, and the most significant impacts on balance are likely to be dynamic in nature, assessing the margin and outlet glacier balance characteristics and mechanisms that affect them is important to understanding the current ice sheet conditions, and predicting the future behavior of the ice sheet as a whole.

In general, the outlet glaciers in the southeast, and south/southwest are showing signs of dramatic thinning. The occurrence of such thinning over such a widespread area raises questions about the stability of these temperate and steep regions of the ice sheet. Similar thinning, though not as substantial is observed in the western side of the ice sheet from Kangerdlugsuup and Rink Isbrae (71°N) to as far north as Humboldt Gletscher (79.5°N) Even parts of Petermann show appreciable thinning, but more data are needed to be conclusive.

Despite the fact that observations are only separated by two years on Ryder Glacier in the north, it shows evidence of being very dynamic with considerable along-flow variability that may be a result of mini-surge behavior. While three glaciers in the northeast show behavior consistent with surging glaciers, the northern ice dome of Kron Prins Christian Dome appears to be thickening – a probable result of its unique local climate characteristics and independent dynamics.

Acknowledgements

This research was supported by NASA's Polar Research Program. We are grateful to the crew of the NASA P-3 aircraft for their efforts in acquiring the data. We also thank R. Mitchell, J. Scott, and A. Waller for their technical support.

References

Abdalati, W., W.B. Krabill, 1999. Application of aircraft laser altimetry to glacier and ice cap mass balance studies, *Archives of the International Society for Photogrammetry and Remote Sensing*, Proceedings of the Workshop in Mapping Surface Structure and Topography by Airborne and Spaceborne Lasers, Lajolla, CA, November 9-11, 1999.

Braithwaite, R.J., 1995. Positive degree-day factors for ablation on the Greenland ice sheet studied by energy-balance modelling, J. Glaciol. 41(137), 153-160.

Bromwich, D.H., Q.-s. Chen, L.-s. Bai, E. Sinclair, and Y. Li., Modeled precipitation variability for the Greenland Ice Sheet"

Joughin, I. S. Tulaczik, S. Fahnestock, R. Kwok, 1996. A mini-surge on the Ryder Glacier, Greenland, observed by satellite radar interferometry. *Science*, **274**(5285), 228-230.

Krabill, W. W. Abdalati, E. Frederick, S. Manizade, C. Martin, J. Sonntag, R. Swift, R. Thomas, W. Wright, and J. Yungel, in press. Greenland ice sheet: high-elevation balance and peripheral thinning, *Science*, in press.

Krabill, W., E. Frederick, S. Manizade, C. Martin, J. Sonntag, R. Swift, R. Thomas, W. Wright, J. Yungel, 1999. Rapid thinning of parts of the southern Greenland ice sheet, *Science*. **283**, 1522-1524.

Krabill, W.B., R.H. Thomas, C.F. Martin, R.N. Swift, E.B. Frederick, 1995. Accuracy of airborne laser altimetry over the Greenland ice sheet, *Int. J. Remote Sens.*, **16**, 1211-1222.

McConnell, J. R., R. J. Arthern, E. Mosley-Thompson, C. H. Davis, R. C., Bales, R. Thomas, J. F. Burkhart, and J. D. Kyne, 2000. Greenland ice sheet elevation changes derived from measured snow accumulation, *Nature*, in press.

Ohmura, A., N. Reeh, 1991. New precipitation and accumulation maps for Greenland, *J. Glaciol.*, **37**, 140-148.

Paterson, W.B., 1994. The Physics of Glaciers, Elsevier Science Ltd. Oxford, 480 pp.

Reeh, N., 1991. Parameterization of melt rate and surface temperature on the Greenland ice sheet . *Polarforschung*, **59**(3), 1989, 113-128.

Reeh, N., C.E. Bøggild, H. Oerter, 1994. Surge of Størstrommen, a large outlet glacier from the inland ice of northeast Greenland, *Geology of North-East Greenland 75°-78°30'N. Rapp. Grønlands Geol. Unders.* edited by Higgins, A.K. **162**, Copenhagen, 201-209.

Rignot, E., 1996. Tidal motion, ice velocity and melt rate of Petermann Gletscher, Greenland, measured from radar interferometry, *J. Glaciol*, **42**, 142, 476-486.

Rignot E.J., S. Gogineni, W.B. Krabill, S. Ekholm, 1997. North and northeast Greenland ice discharge from satellite radar interferometry. Science, **276** (5314) 934-937.

Thomas, R.H., W. Abdalati, T.L. Akins, B.M. Csatho, E.B. Frederick, S.P. Gogineni, W.B. Krabill, S.S. Manizade, E.J. Rignot, 2000. Substantial thinning of a major east Greenland outlet glacier, *Geophys. Res. Lett.*, **27**(9), 1291-1294.

Thomas, R.H., C.H. Davis, E. Fredrick, S. Manizade, W. Krabill, J. McConnell, and J. Sonntag, submitted. 20-year time series of Greenland ice-sheet thickness change from radar and laser altimetry, *Polar Geography*, submitted.

Van der Veen, C.J., 1993. Interpretation of short-term ice–sheet elevation changes inferred from satellite altimetry. *Clim. Change*, **23**, 383-405.

Van der Veen, C.J., 1999. Fundamentals of Glacier Dynamics, A.A. Balkema Publishers, Rotterdam, Netherlands, 462 pp.

Weidick, A., 1985, Review of glacier changes in west Greenland, *Z. Gletscherkd. Glazialgeol.*, **21**, 301-309.

Weidick, A., 1995. *Satellite Image Atlas of Glaciers of the World: Greenland*, United States Geological Survey, professional paper 1386-C, edited by R.S. Williams, J. Ferrigno, U.S. Government Printing Office, Washington, DC, 141pp.

Figure Captions:

Figure 1. Overview of the Greenland ice sheet, showing where surveys were flown, and locations of various coastal weather stations used in the study.

Figure 2. Observed elevation change rates for each surveyed area. Thinning is shown in red, and thickening is shown in black. Also shown are the elevation changes derived from the PDD anomaly for each coastal station (m/yr). Detailed plots for each transect in each of the different regions, EC, S, WC, NW, NE are shown in Figures 3 through 7 respectively.

Figure 3. Elevation change rates (thick gray points) and elevations (thick black points) along transects at outlet glaciers and ice margin at locations in the central eastern section of the ice sheet (Shown in Fig. 2). Also shown are the typical ablation rates (thin black lines) and ablation anomalies (thin dashed line) for the flight lines. The ablation rates are based on Reeh's (1991) positive degree day (PDD) model and the PDD factors of 3 mm/yr and 8 mm/yr for snow and ice respectively [Braithewaite, 1995], and are expressed in terms of snow height. The anomalies are calculated from 20 years worth of coastal station temperature data, as described in the text.

Figure 4. Elevation change rates (thick gray points), elevations (thick black points), ablation rates (thin black lines), and ablation anomalies (dashed black line) along transects at outlet glaciers and ice margin at locations in the southern section of the ice sheet (Shown in Fig. 2).

Figure 5. Elevation change rates (thick gray points), elevations (thick black points), ablation rates (thin black lines), and ablation anomalies (dashed black line) along transects at outlet glaciers and ice margin at locations in the western section of the ice sheet (Shown in Fig. 2).

Figure 6. Elevation change rates (thick gray points), elevations (thick black points), ablation rates (thin black lines), and ablation anomalies (dashed black line) along transects at outlet glaciers and ice margin at locations in the north/northwest section of the ice sheet (Shown in Fig. 2). Only the down-glacier flights are shown for Humboldt.

Figure 7. Elevation change rates (thick gray points), elevations (thick black points), ablation rates (thin black lines), and ablation anomalies (dashed black line) along transects at outlet glaciers and ice margin at locations in the northeast section of the ice sheet (Shown in Fig. 2).

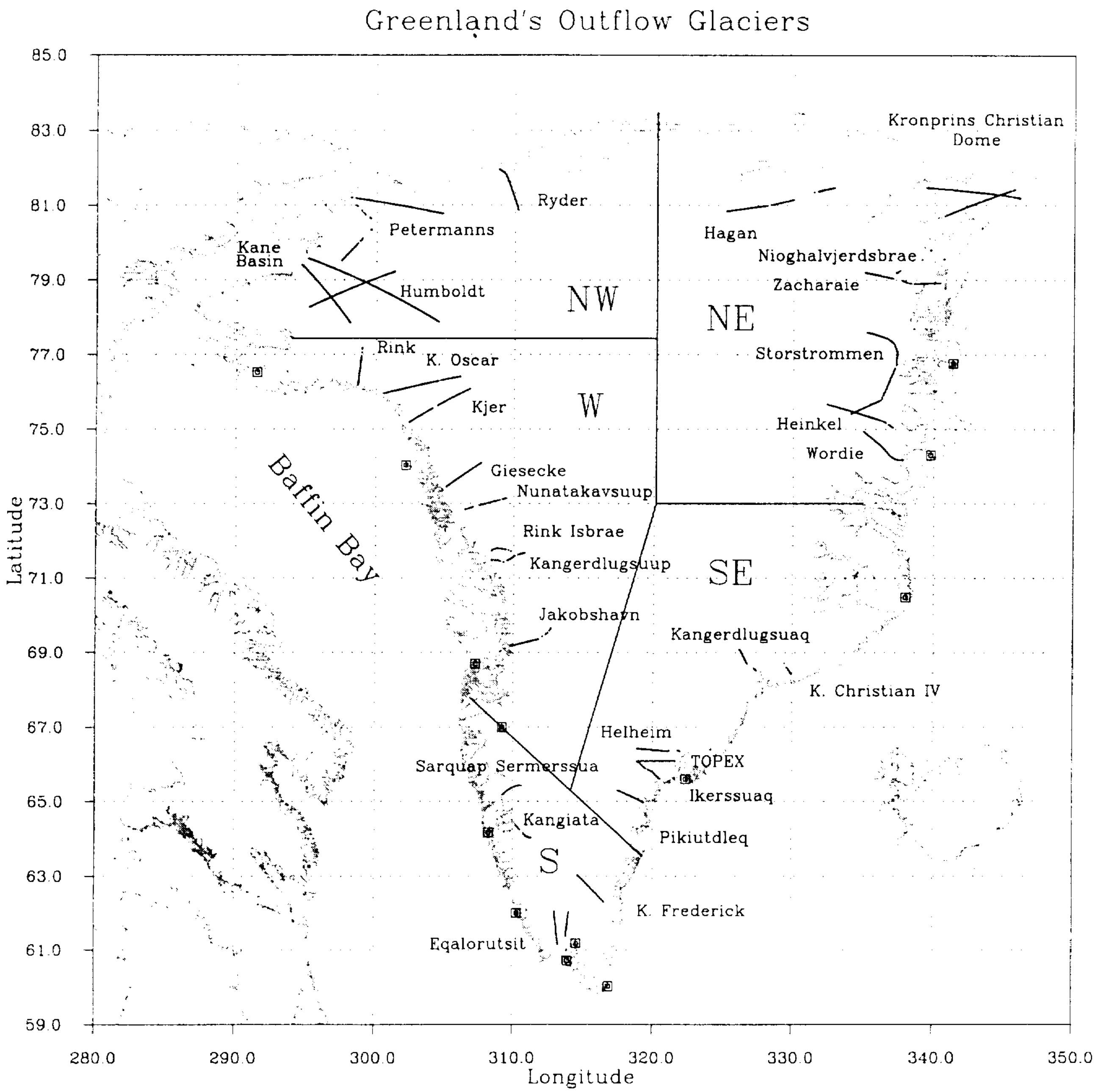

Greenland's Outflow Glaciers
Kronprins Christian Dome
Ryder
Petermanns
Kane Basin
Humboldt
NW
Hagan
Nioghalvjerdsbrae
Zacharaie
NE
Rink
K. Oscar
Storstrommen
Kjer
W
Heinkel
Wordie
Baffin Bay
Giesecke
Nunatakavsuup
Rink Isbrae
Kangerdlugsuup
SE
Jakobshavn
Kangerdlugsuaq
K. Christian IV
Helheim
TOPEX
Sarquap Sermerssua
Ikerssuaq
Kangiata
Pikiutdleq
S
K. Frederick
Eqalorutsit
Latitude
Longitude
85.0
83.0
81.0
79.0
77.0
75.0
73.0
71.0
69.0
67.0
65.0
63.0
61.0
59.0
280.0
290.0
300.0
310.0
320.0
330.0
340.0
350.0

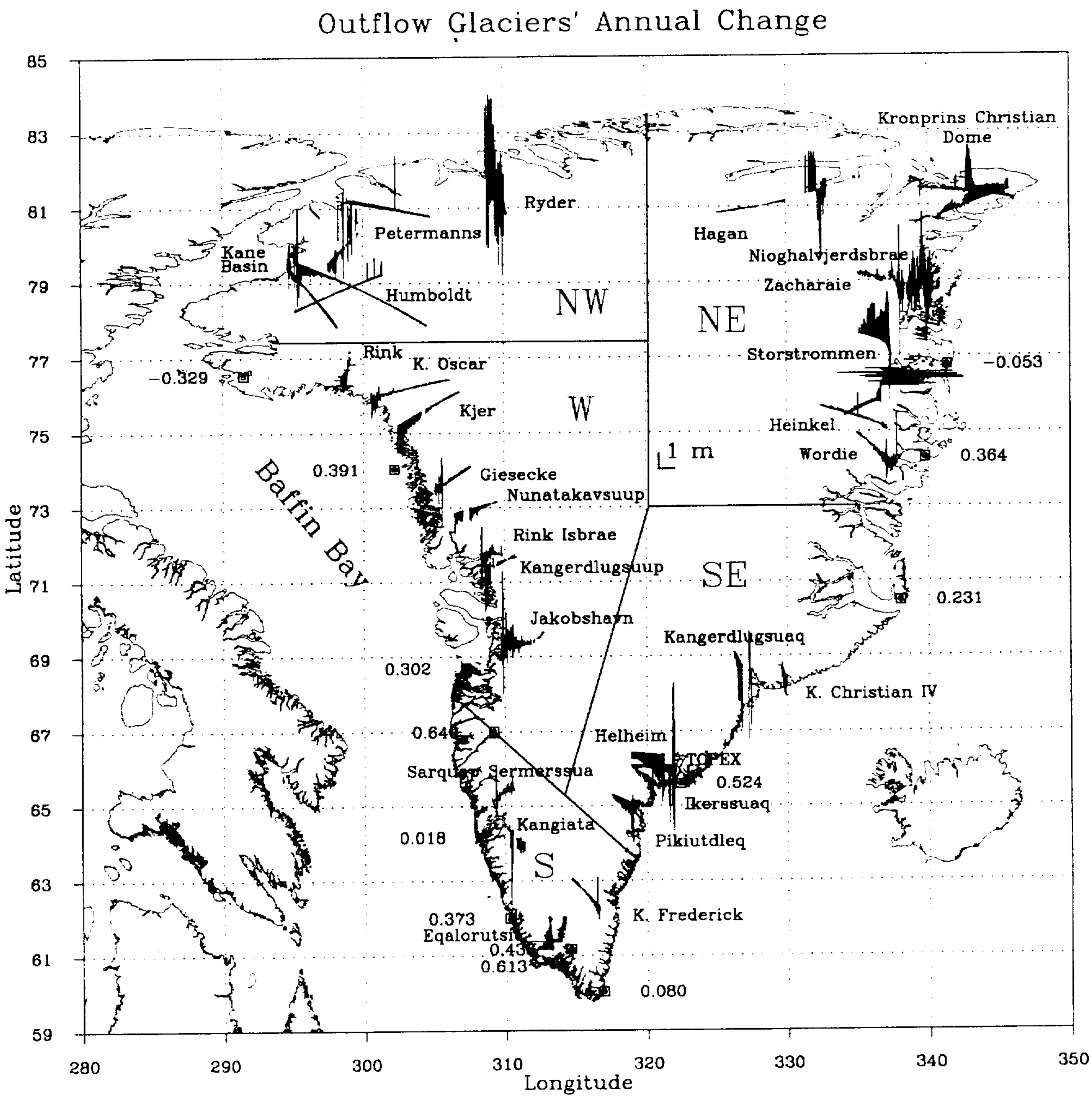
Outflow Glaciers' Annual Change
Latitude
Longitude
85
83
81
79
77
75
73
71
69
67
65
63
61
59
280
290
300
310
320
330
340
350
Kronprins Christian
Dome
Ryder
Petermanns
Kane
Basin
Humboldt
NW
Hagan
Nioghalvjerdsbrae
Zacharaie
NE
Storstrommen
-0.053
Rink
K. Oscar
-0.329
Kjer
W
Heinkel
Wordie
0.364
1 m
0.391
Giesecke
Nunatakavsuup
Baffin Bay
Rink Isbrae
Kangerdlugsuup
SE
0.231
Jakobshavn
Kangerdlugsuaq
0.302
K. Christian IV
Helheim
TOPEX
0.524
Sarqu Sermerssua
Ikerssuaq
Kangiata
Pikiutdleq
0.018
S
K. Frederick
0.373
Eqalorutsi
0.613
0.080

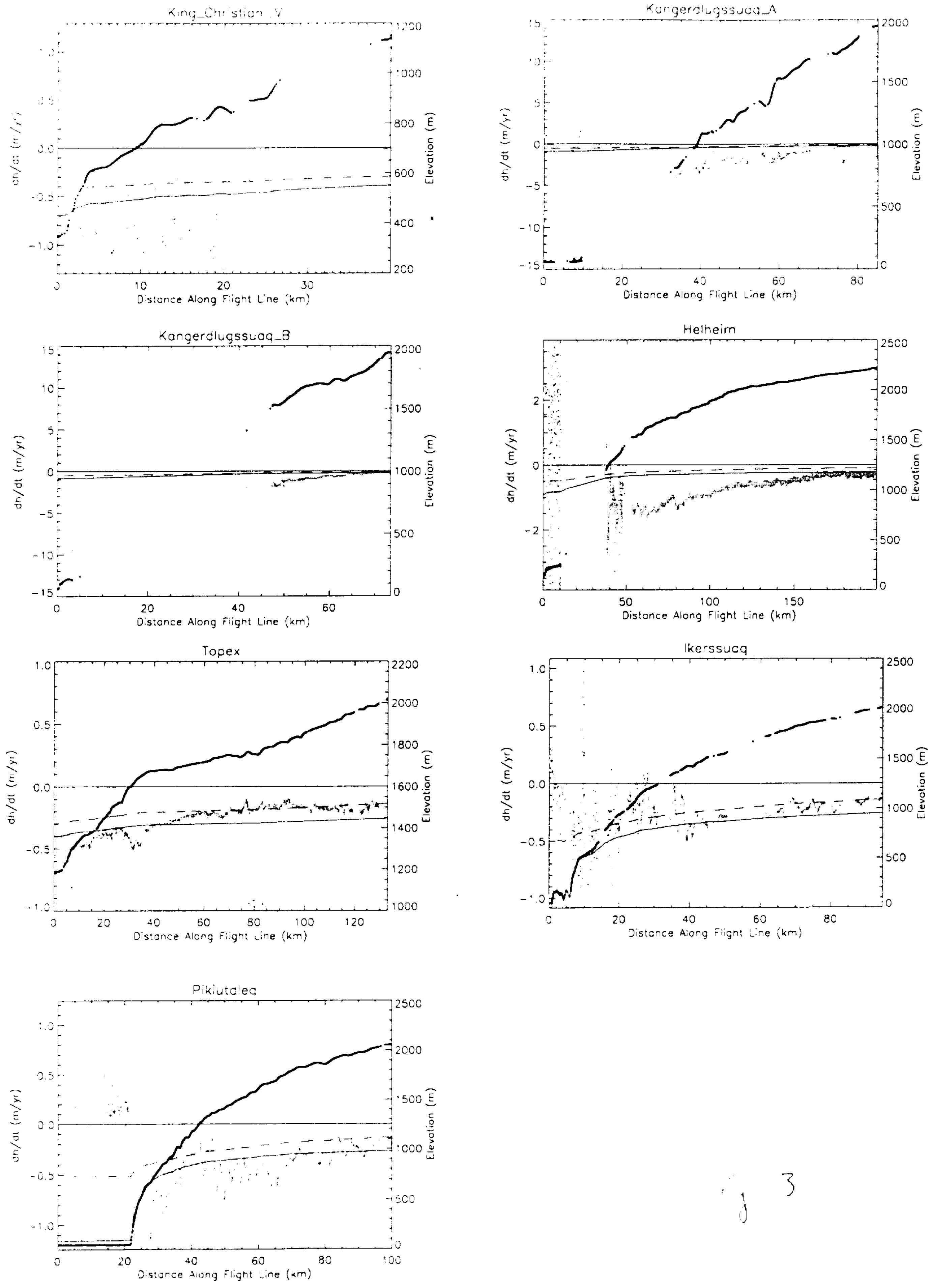
King_Christian_V
Kangerdlugssuaq_A
Kangerdlugssuaq_B
Helheim
Topex
Ikerssuaq
Pikiutdleq
dh/dt (m/yr)
Elevation (m)
Distance Along Flight Line (km)

Fig 3

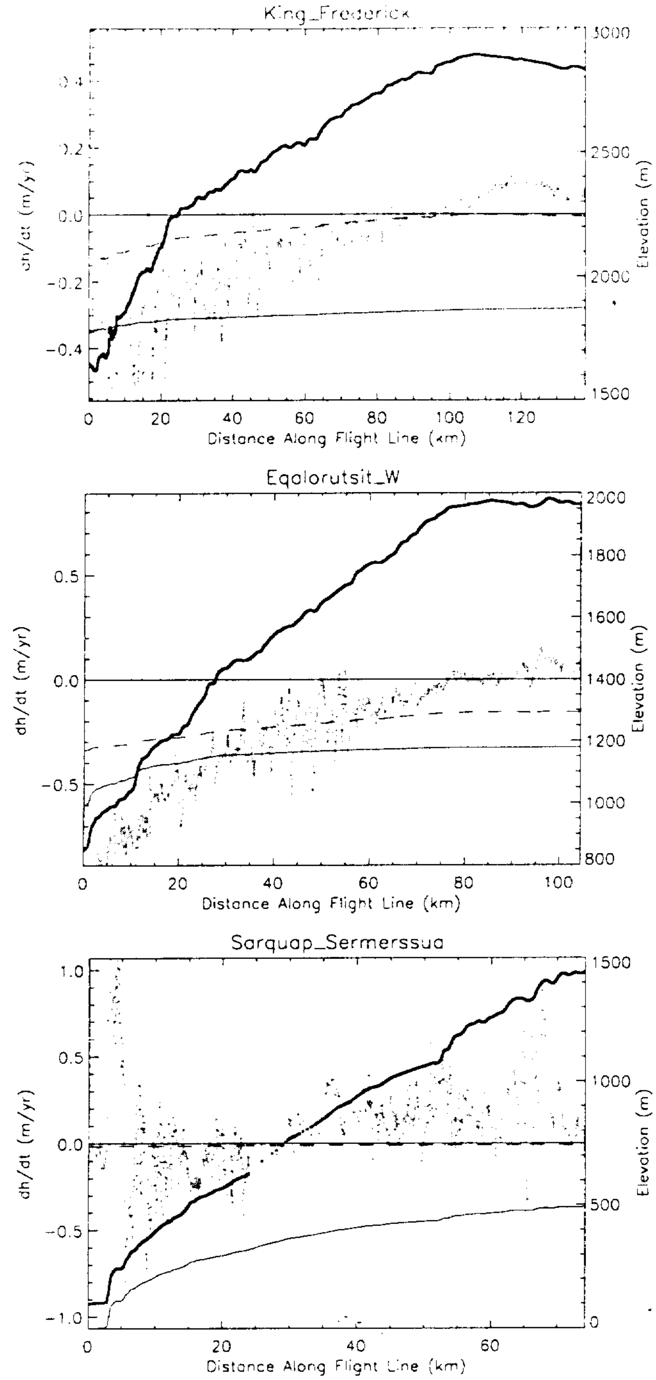
King_Frederick
dh/dt (m/yr)
Elevation (m)
Distance Along Flight Line (km)
Eqalorutsit_E
dh/dt (m/yr)
Elevation (m)
Distance Along Flight Line (km)
Eqalorutsit_W
dh/dt (m/yr)
Elevation (m)
Distance Along Flight Line (km)
Kangiata_Nunata_Sermia
dh/dt (m/yr)
Elevation (m)
Distance Along Flight Line (km)
Sarquap_Sermerssua
dh/dt (m/yr)
Elevation (m)
Distance Along Flight Line (km)

Fig 4

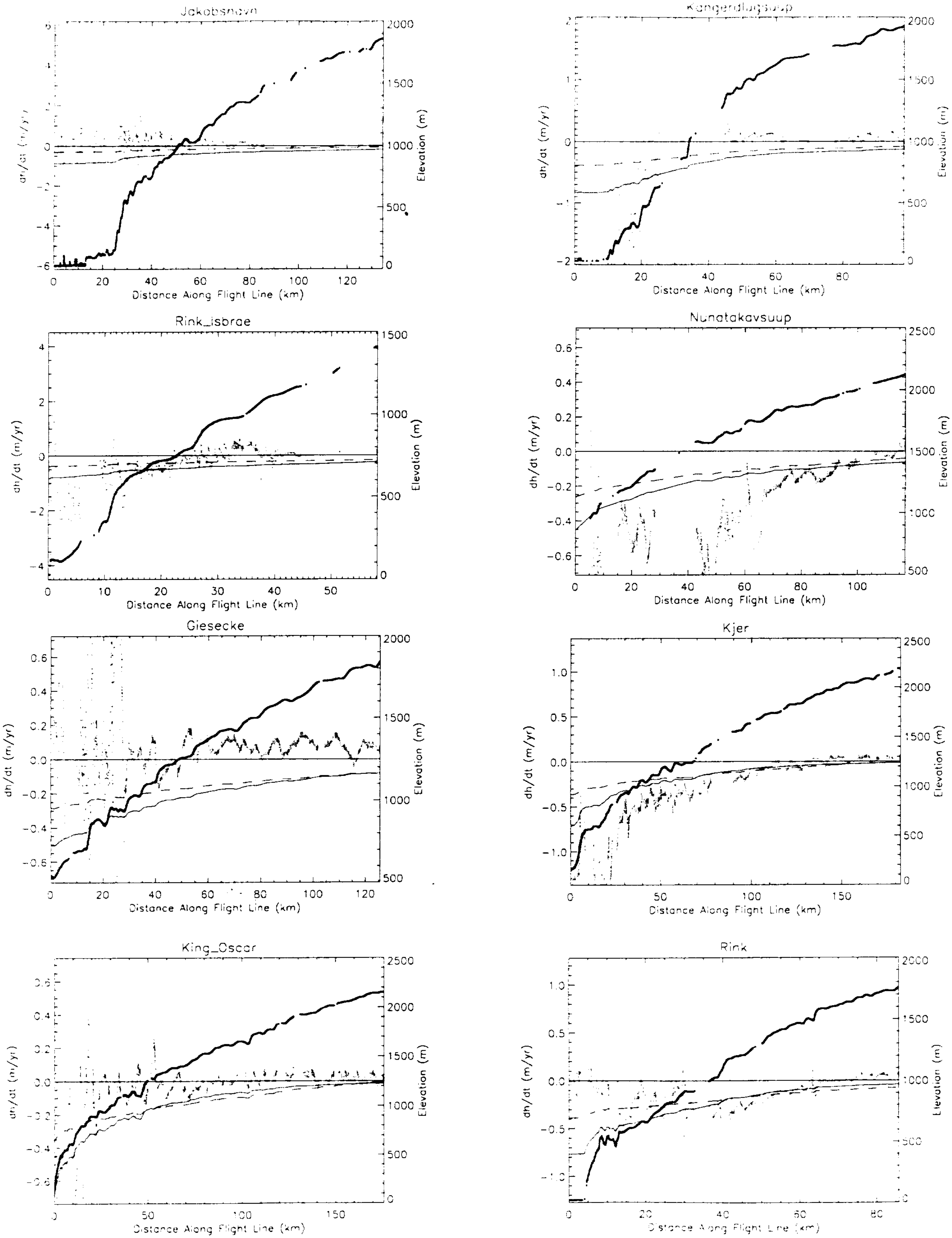
Jakobsnavn
dh/dt (m/yr)
Elevation (m)
Distance Along Flight Line (km)
Kangerdlugssuup
dh/dt (m/yr)
Elevation (m)
Distance Along Flight Line (km)
Rink_isbrae
dh/dt (m/yr)
Elevation (m)
Distance Along Flight Line (km)
Nunatakavsuup
dh/dt (m/yr)
Elevation (m)
Distance Along Flight Line (km)
Giesecke
dh/dt (m/yr)
Elevation (m)
Distance Along Flight Line (km)
Kjer
dh/dt (m/yr)
Elevation (m)
Distance Along Flight Line (km)
King_Oscar
dh/dt (m/yr)
Elevation (m)
Distance Along Flight Line (km)
Rink
dh/dt (m/yr)
Elevation (m)
Distance Along Flight Line (km)

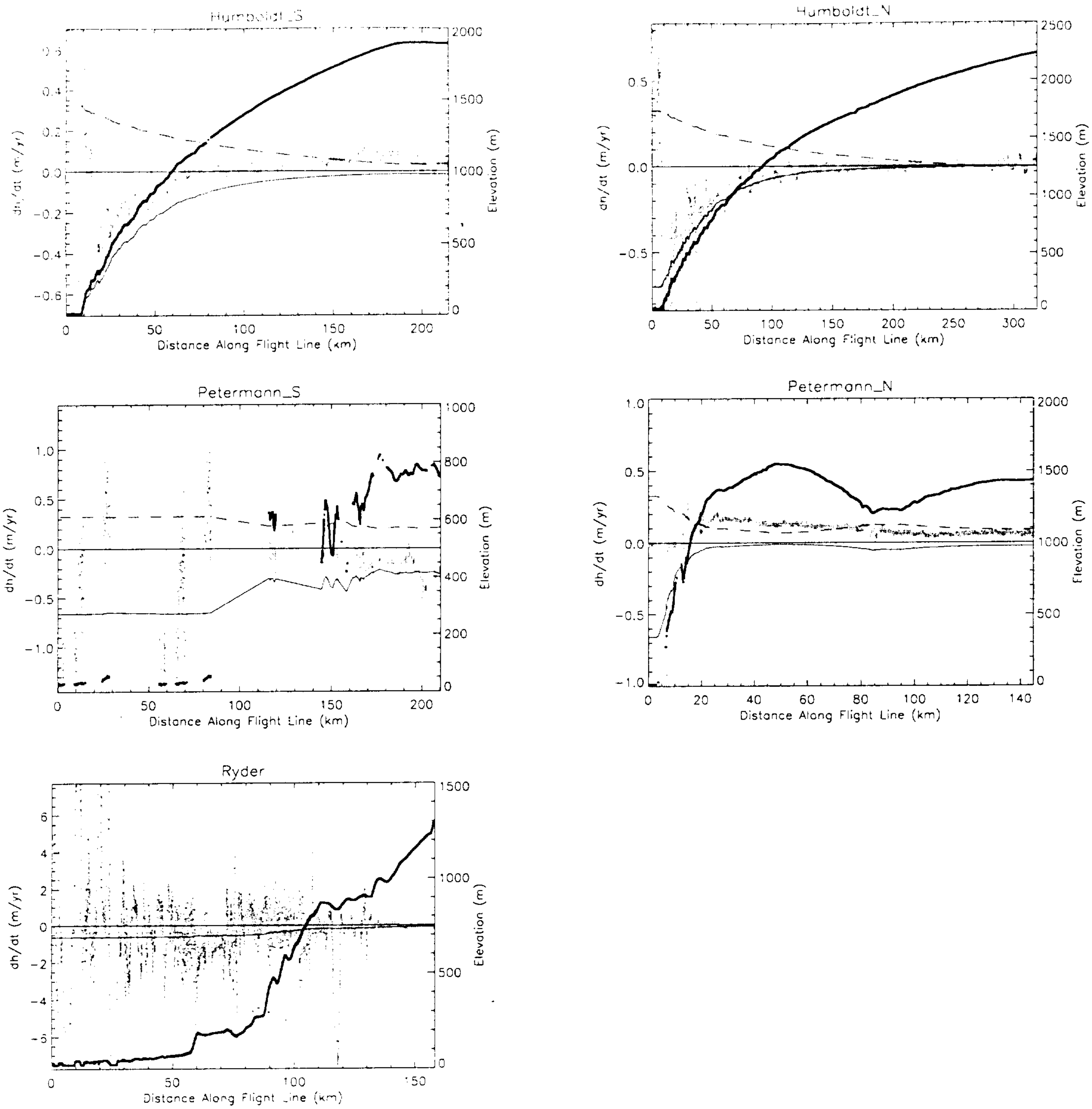
Humboldt_S
Humboldt_N
Petermann_S
Petermann_N
Ryder
dh/dt (m/yr)
Elevation (m)
Distance Along Flight Line (km)

Fig 6

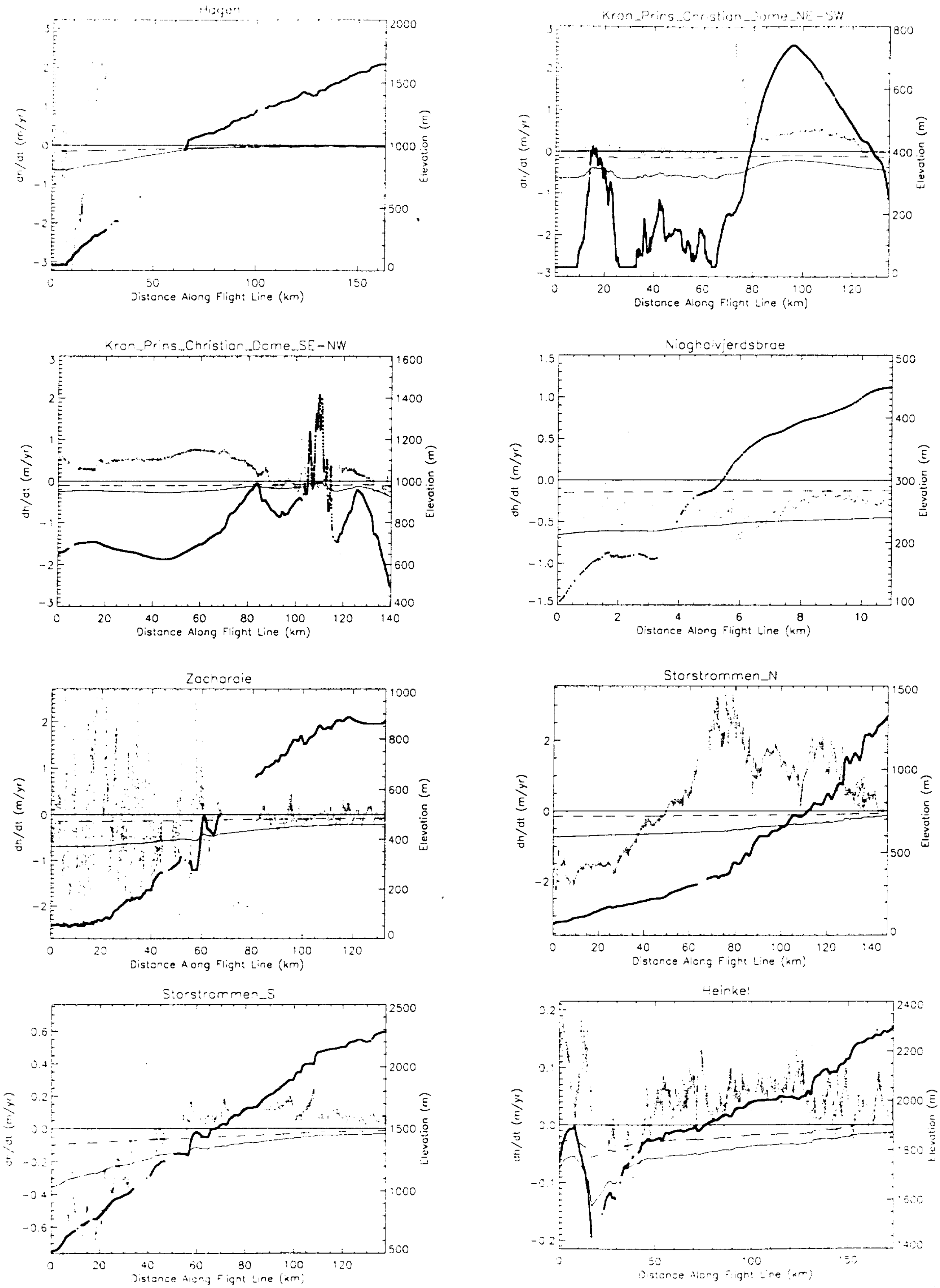
Hagen
dh/dt (m/yr)
Elevation (m)
Distance Along Flight Line (km)
Kron_Prins_Christian_Dome_NE-SW
dh/dt (m/yr)
Elevation (m)
Distance Along Flight Line (km)
Kron_Prins_Christian_Dome_SE-NW
dh/dt (m/yr)
Elevation (m)
Distance Along Flight Line (km)
Nioghalvjerdsbrae
dh/dt (m/yr)
Elevation (m)
Distance Along Flight Line (km)
Zacharaie
dh/dt (m/yr)
Elevation (m)
Distance Along Flight Line (km)
Storstrommen_N
dh/dt (m/yr)
Elevation (m)
Distance Along Flight Line (km)
Storstrommen_S
dh/dt (m/yr)
Elevation (m)
Distance Along Flight Line (km)
Heinkel
dh/dt (m/yr)
Elevation (m)
Distance Along Flight Line (km)

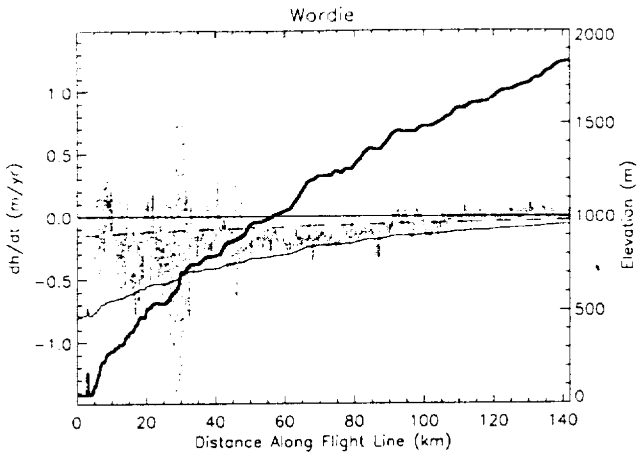
Wordie
dh/dt (m/yr)
Elevation (m)
Distance Along Flight Line (km)
1.0
0.5
0.0
-0.5
-1.0
2000
1500
1000
500
0
0
20
40
60
80
100
120
140

Fig 7 (cont'd)